

Facile Preparation of Porous Silicon from Silver-Assisted Chemical Etching Method on Silicon

Jin Chen^{*}, Xueming Li, Wenjing Yang, Yixuan Mou, Anqi Li, Yuting Xie, Yali Wang and Peng Xu

College of Chemistry and Chemical Engineering, Chongqing University, Chongqing, 401331, China

^{*}Corresponding author e-mail: 2454795265@qq.com

ABSTRACT. The porous silicon (PS) has many promising applications in silicon technologies development and integrated MEMS machining. Currently, many reports show that metal-assisted chemical etching can be a potential substitute for the electrochemical method. To broaden the fabrications and applications of porous silicon (PS), this research investigated the method based on silver-assisted chemical etching. Silvers particles were reduced by ascorbic acid under PVP protection, whose proper dosage was discussed. With the existence of oxidation component H₂O₂ and etchant HF, a silicon substrate can be etched into regular holes. The characterization results show that the silver-assisted etching structures may be spatially adjusted by disperse silver nanoparticles deposition. Furthermore, those porous silicon chips were proved to be energetic after dipping the certain concentration of nitrate, for violent exothermic when ignited. To sum up, controllable silver-assisted chemical etching provides a facile technique to fabricate PS that can be employed to realize wider manufacture.

KEYWORDS: Porous silicon, silver-assisted chemical etching

1. Introduction

Since the 1950s porous silicon (PS) material was accidentally discovered by Uhlir [1], it has attracted many investigations to utilize its advantage like high surface area and reactivity. There are lots of potential applications for good compatibility with silicon technologies such as energy [2, 3], various sensors [4, 5] and so on. Explosion merit of nanostructured porous Si from the electrochemical method was first reported by Mikulec [6], which can combust or explode when filled with oxidizers. Then many research have been carried out on this topic to develop a promising energetic material for ecologically pyrotechnic systems in the current semiconductor industry [7, 8]. Substantial works have been devoted to improving

superior performance of PS, while the vast applications for practical devices are still limited to synthesis methods. Concerning massive manufacturing method, PS is mainly formed by electrochemical etching (anodic dissolution) treatment of a silicon wafer in hydrofluoric-acid (HF) solutions, which consumes lots of energy and inappropriate for mass production as well. So it is significant to develop more efficient and simpler methods for mass production.

The original proposal of metal-assisted chemical etching (MACE) method was discovered by Dimova.Malinovska [9] that p-type Si loaded with Al film was etched into porous holes, then the pioneering work can be traced to Li and Bohn who proposed more details in 2000 [10]. Soon the topic has been extensively studied and in 2008 Huang, Z. [11] gave an incisive introduction review about this technique. In a typical metal-assisted etch process, metal material particles or dots remain on the top surface could act as a catalyst engine when it etches in aqueous HF solutions. Unlike electrochemical etching techniques, it does not require any external power supply because current flux can be continuously provided from the reduction of H_2O_2 at the metal nanoparticles and anodic dissolution of bulk Si [12]. Moreover, compared with electrochemical corrosion where holes injection spread over the whole surface, holes of MACE can be so concentrated around the interface due to the catalytic properties that bring uniform structure [13]. Nowadays, this method has been extensively applied for the fabrication of dimensional Si nanostructures for high efficiency and controllable fabrication [14-16]. For example, it was mainly proposed to produce large-area Si nanowire (SiNWs) arrays from noble metal-assisted etching such as Au [17, 18], Ag [19, 20], Pd [21], Pt [22] and so on.

From the above, it is known that the majority of MACE investigations focused on silicon nanowires in previous work. Although substantial work has been devoted to metal-assisted Si chemical etching, little attention has been conducted on applying for porous silicon than SiNWs. Moreover, few studies of PS by MACE either need complicated procedures, high-cost instrumentations or exhibit poor spatial ordering and broad diameter distribution due to the direct deposition of metal salt. In this work, we tried direct synthesize of silver deposition to acquire porous silicon based on silver-assisted chemical etching (SACE), the results suggested that silver (Ag) nanoparticles by the controllable reduced method can be used to fabricate porous silicon with deep and uniform holes covered. On the other hand, the SACE method may be a promising maskless nanofabrication technology due to its low cost, simplicity and so on, which offers a cheap and convenient method to extend the fabrication of PS and broaden the application field of porous silicon soon.

2. Experimental

2.1 Materials

Hydrofluoric acid (HF, 40%, AR), ethanol (EtOH, 99.5%, AR), acetone (AR), hydrogen peroxide (H_2O_2 , 35%, AR), hydrochloric acid (HCl, AR), ammonia (NH_4OH , 35%, AR), nitric acid (HNO_3 , AR), N,N-Dimethylacetamide (DMAC,

AR), silver nitrate (AgNO_3 , AR), ascorbic acid ($\text{C}_6\text{H}_8\text{O}_6$, AR) were purchased from Kelong Chemical Reagent Co., Ltd. PVP- K_{30} (poly vinyl-pyrrolidone, Mw~40,000, AR), gadolinium nitrate hydrate ($\text{Ga}(\text{NO}_3)_3$, AR) were purchased from Aladdin Chemical Reagent Co., Ltd. The silicon wafers were purchased from Emei Semiconductor Material Institute (China), which was single-side polished crystalline (1 0 0) p-type boron-doped with a resistivity of 0.01–0.02 $\Omega \cdot \text{cm}$ (thickness~525 μm).

2.2 Pretreatment of Si

Si wafers were cleaved into 1×1 cm² samples and installed onto the special made Teflon/PTFE equipment, which composed of PTFE etching part, an O-ring and iron plate in the bottom to seal up. The pre-treatment was as follows: First, those chips were ultrasonically cleaned 5 min in acetone and ethanol to remove organic deposits, respectively. Then oxide layer on the surface were removed with 10% HF solution 10 min and RCA solution ($\text{H}_2\text{O} : \text{H}_2\text{O}_2 : \text{NH}_4\text{OH} = 5:1:1$, $\text{H}_2\text{O} : \text{H}_2\text{O}_2 : \text{HCl} = 5:1:1$) 5 min, after that deionized water washing is vital.

2.3 Preparation of Ag particles

Ag nanoparticles (AgNPs) generated from chemical deposition by AgNO_3 (3 mM = 3 mmol) in the mixture of reductant Ascorbic acid (1 mM, 5 mM, 10 mM) with certain volume ratio, capping agents PVP- K_{30} (dissolved in ethylene glycol-EG) at room temperature (~20 °C) for seconds, then the excess Ag^+ in the solution were washed with deionized water (Di-water, double distilled).

2.4 Fabrication of energetic PS

After the electroless metallization, the AgNPs coated Si wafers were etched in aqueous solutions containing HF (mW=40%), H_2O_2 (mW=35%) at different volume ratios and auxiliary wetting agents such as deionized H_2O , DMAC for different times (marked as t). Then, the Si chips were detached and soaked in HNO_3 (4 M) to remove the residual AgNPs, cleaned with de-ionized water several times. Finally, 5 μL $\text{Ga}(\text{NO}_3)_3$ oxidizer (1 M) was dripped onto fresh PS sample and infiltrating about 2min, then superfluous oxidizer should be wiped and chips were dried in vacuum oven at 50 °C for a couple of hours.



Figure. 1 Schematic illustrations of the whole fabrication process through two-step; Silver Assisted Etching method and the main equipment diagram

2.5 Characterization

Characterization of AgNPs were conducted by particle size analyzer (Brookhaven NanoBrook Omni), digital microscope (Zeiss Axio Scope), Field Emission Scanning Electron Microscope (HR-SEM, JSM-7800F, JEOL). The morphological structure characterizations of PS were examined by SEM, and the energetic explosion performance were ignited with resistive heating spark and tested by Electric spark detonator and camera.

3. Results and discussion

3.1 Ag nanoparticle deposition

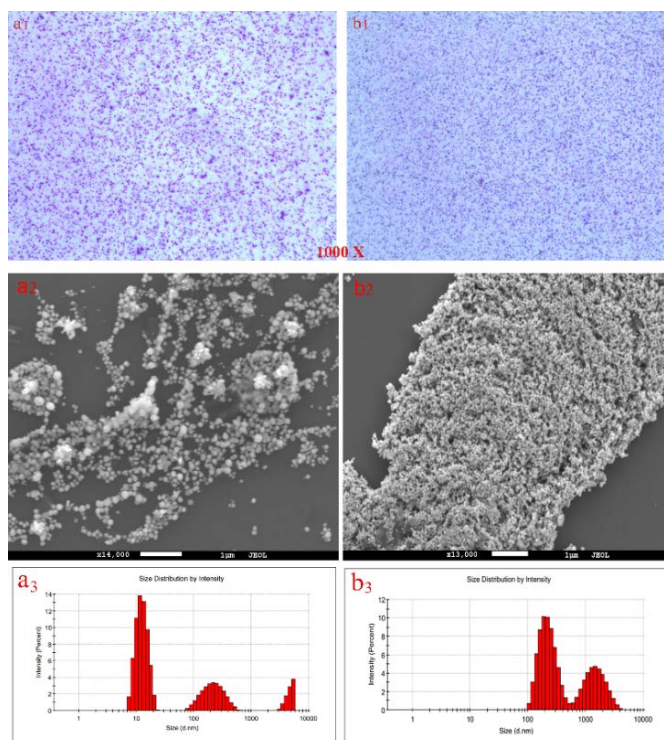


Figure. 2 Microscope images, SEM pattern and their particle size distribution histograms results of surface after Ag reduced deposition on silicon surface at different volume ratio ($AgNO_3$: Ascorbic)
 (a1, a2, a3) 0.5 mL $AgNO_3$ +1 mL Ascorbic,
 (b1, b2, b3) 1 mL $AgNO_3$ +1 mL Ascorbic

After 5 min metallization and growth from 3 mM $AgNO_3$ reduced by 0.5M ascorbic acid as [Eq. (1)], the Si surface is loaded by plentiful silver. Figure.2 (a1), (b1) show the microscope images of the deposition layer, which can be observed that there exist many distributed tiny dots on the Si surface.

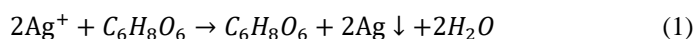


Figure.2 (a2), (b2) show SEM morphology of substantial Ag particles of the early plan (direct chemical reduction of $AgNO_3$ in aqueous ascorbic acid without PVP addition), where massive Ag particles gather like nano-clusters and shroud the surface separately, which can be explained from the multiple size distribution

figures (a3), (b3). As reported by the research of [23, 24], the morphology of deposited metals is determined not only by ionic salt, reductant and their molarity, but also solution polarity, deposition time, temperature, the pre-treatment of Si wafer and so on. To explain that result, solution tension and surface energy in the growth of Ag nuclei shall be first adjusted.

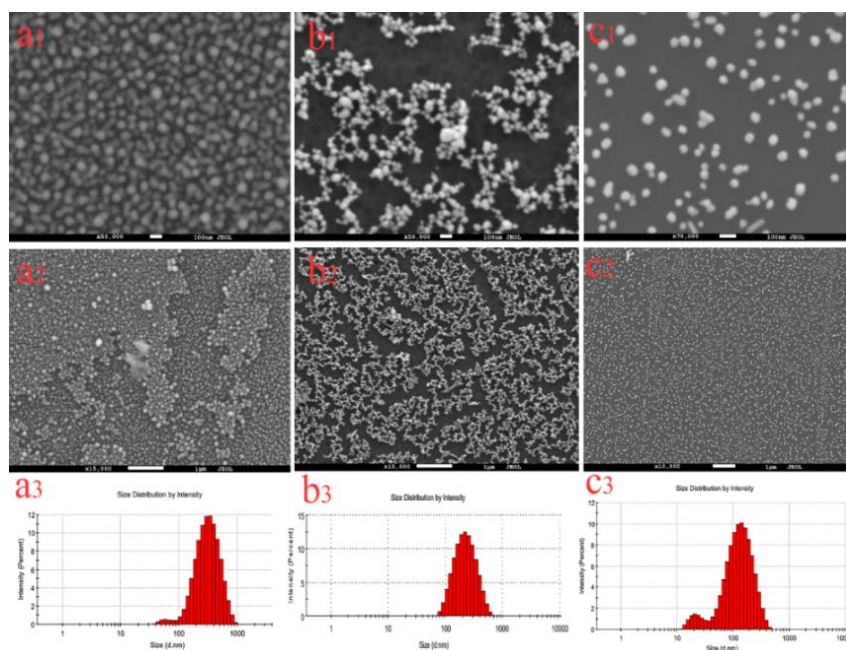


Figure. 3 SEM photos and their particle size distribution histograms results of different PVP dosage

(a1, a2, a3) 0.5 mL AgNO_3 + 1 mL Ascorbic + 0.2 mL PVP;

(b1, b2, b3) 0.5 mL AgNO_3 + 1 mL Ascorbic + 0.8 mL PVP;

(c1, c2, c3) 0.5 mL AgNO_3 + 1 mL Ascorbic + 2.0 mL PVP.

In order to solve the rough accumulation deposition and optimize the morphology of these particles, we studied different synthesis scheme of silver nanoparticles (AgNPs) [25, 26]. Then we added a certain amount of PVP (5mM, dissolved in ethylene glycol) as a distribution component into the solution system (1mM AgNO_3). With the increase of PVP, these particles gradually separated and size shrunk as observed from SEM Fig.4 a1-c2. The size distribution histograms also showed that the surface can be successfully suffused with abundant isolate AgNPs of similar size spheres around 100 nm.

According to the theory of [27], because PVP molecules have a structure of long polyvinyl skeleton with pyrrolidone as polar groups which will strongly adsorb on

the silver surface to form polymer@Ag coordination, it is these complexes that can prevent the AgNPs from being agglomerated, illustrated as follows Scheme.1.

In conclusion, the introduction of PVP plays a crucial role as surfactant and dispersant in the reaction system, they not only reduce tension to avoid accumulation but increase the wettability of the Si surface to enable better Ag nuclei distribution.

3.2 Si etching

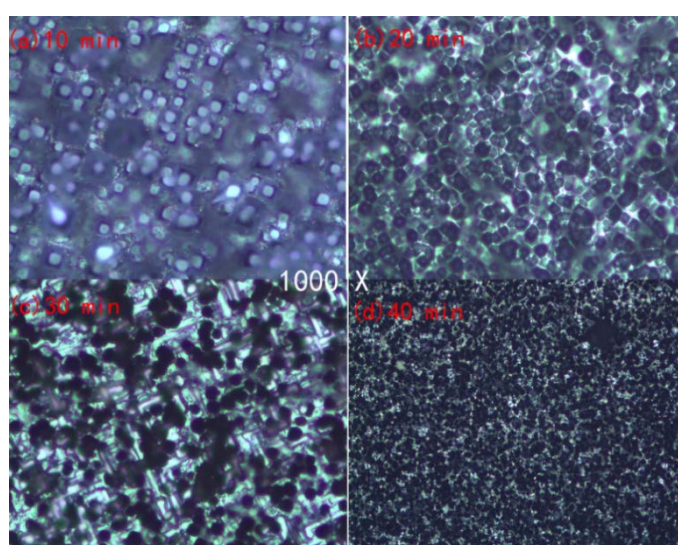


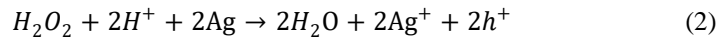
Figure. 4 Microscope images of corrosion process on the silicon surface

Before etching the Ag covered silicon, the chips should first be cleaned with ethanol and water to remove solution remaining, then immersed in etchant HF and H₂O₂ (5 mL HF (40%), 1 mL H₂O₂ (10%), 1 mL H₂O, t =20 min). When the reaction began spontaneously, there were many bubbles emerged from the interface between the silicon surface and solution. We recorded micro appearance change of the surface with digital microscope every 10 min. As can be seen on the above 4 pictures (Fig.4), these distributed silver particles gradually sunk with etching times but stable, finally the silicon layer became dark and porous as well.

To illustrate this phenomenon, various mechanisms for this has been proposed since the first report of MACE a decade ago [12, 28, 29]. Considering that the mechanism is still not certain, we quote one comprehensive explanation of mechanism proposed by Chartier[12], which appears to be generally applicable of them to illustrate the whole process as follows:

First, few Ag^+ ions may start to nucleate on the defective sites of Si surface after pretreatment or mainly produced by reducing agent [Eq. (1)], then takes seconds to grow into proper Ag particles.

Second, after adding H_2O_2 and HF, a localized h^+ (free holes) could be created in the proximity of Ag particles because of the oxidation of AgNPs by H_2O_2 (or H_2O_2 is catalytically reduced at the Ag nanoparticles). In the meanwhile, AgNPs inject plenty holes (h^+) into the Si [Eq. (2)] because of different Fermi levels or electronegativity between them. Herein, the metal acts as a charge transfer bridge between the silicon and the oxidizers. In other words, H_2O_2 locally oxidizes Ag to Ag^+ so etching tends to occur in the vicinity of the metal due to the higher concentration of h^+ , as if H_2O_2 acts as a driving force of the whole etching.



Third, h^+ are consumed at the HF/Si interface in the oxidation from Si^0 to Si^{4+} as h^+ are necessary for the oxidation of silicon, then dissolved into H_2SiF_6 by HF [Eq. (3)] and released H_2 bubbles. In the meanwhile, re-produced Ag^+ ions can quickly capture electron near the Ag/Si interface and thus recovered into the original Ag. In this case, etching is localized around AgNPs, and then Ag particles are trapped in Nano-pits created by themselves, thus continuous vertical etching leading to tunnels into Si wafer.

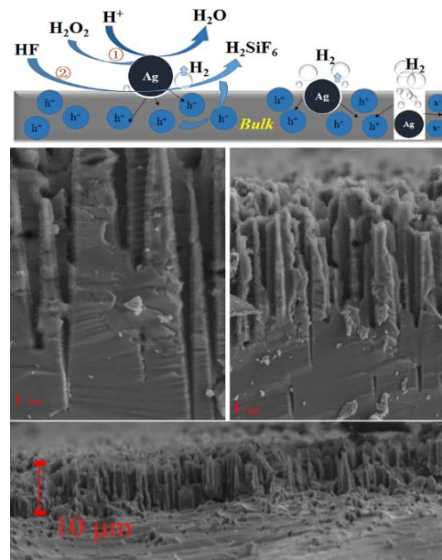
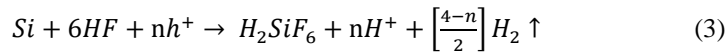


Figure. 5 Visualization of the mechanism in MACE and SEM cross-section image of Ag loaded p-type (1 0 0) Si sample etched in HF– H_2O_2 – H_2O (5:1:1)

As cross-section of the holes array displayed in Figure.5, which confirms the schematic diagram of the mechanism above. In principle, the fabrication of Si via the MACE process is intrinsically microscopic galvanic corrosion. For the shortest charge-transport distance and unique catalytic surface property of Ag nanoparticles, an enhanced cathodic reaction occur preferentially at the noble metal surface of reducing the oxidizing agent from the etching solution. Simultaneously, an anodic reaction occurs on the metal/Si interface, then the oxidized Si is dissolved into an aqueous etching complex. Owing to an anodic etching of Si below the metal/Si interface proceeds much faster than the etching of bare Si and the wall of already etched structures. As a consequence, it seems that each spherical AgNPs could work as a self-propelled engine or a catalytic “drilling bit” to promote the formation of vertical pores and further porous Si. Considering that well-separated Ag particles sink along the silicon surface and finally form separated holes, so it is feasible to fabricate porous silicon.

3.3 Porosification and Energetic PS characterization

To acquire the final PS, these chips need to be soaked in dilute nitric acid several minutes to solute the silver particles at the bottom of each hole. After that, the chips were washed with Di-water and ethanol then dried in a vacuum oven at 30°C for 20min.

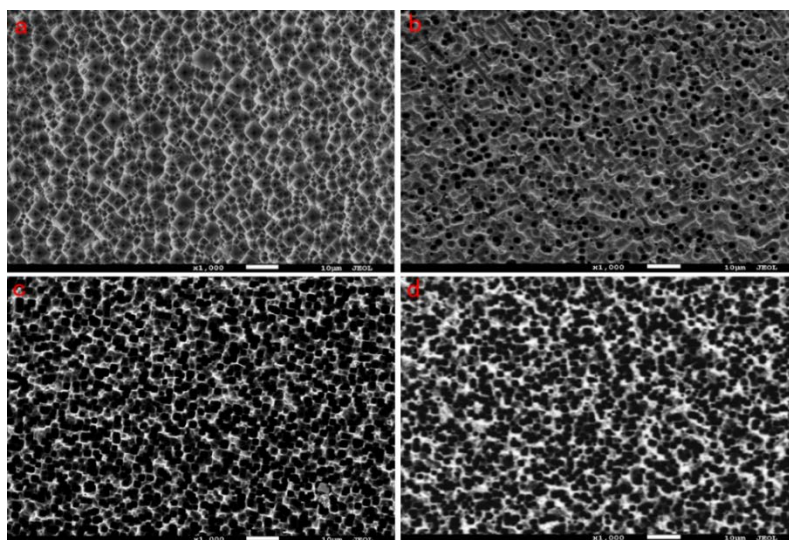


Figure. 6 SEM plan images of Ag covered and assisted-etching of silicon surface at different operation condition:

- (a) 5 mL HF (40%), 1 mL H_2O_2 (10%), 1 mL H_2O , $t=20$ min
- (b) 5 mL HF (40%), 1 mL H_2O_2 (10%), 1 mL DMAC, $t=20$ min
- (c) 5 mL HF (40%), 1 mL H_2O_2 (10%), 1 mL DMAC, $t=40$ min
- (d) 5 mL HF (40%), 1 mL H_2O_2 (35%), 1 mL DMAC, $t=20$ min

As the SEM characterization of Figure.4, Figure.6 (a) demonstrates a porous morphology after etching with separated particles deposition, which confirms the importance of dispersity before corrosion. In other word, the surface coverage and size of AgNPs influence largely the etching characteristics.

To further regular the PS structure and unveil the influence of etchant on the porosification process, we explored several variables of corrosion. As shown in the above four SEM photos in Figure.6, which gives a whole view of porous Si whose surface was covered with plentiful corrosion holes under 5 μm diameter spread independently, where had been coated by separated particles before etching. When (a) compared to (d), the latter shows more deep and round holes than etching in aqueous system, which implies that etching solvent can influence the morphology by controlling the tension of the solution and stability of Ag. And the differences between Figures (b). (c). (d) can be concluded as the H_2O_2 concentration and etch time, two main variables involved in the PS fabrication. According to the survey of [20], as the increase of H_2O_2 concentration and corrosion time, the cathode reaction of H_2O_2 on Ag particles was so active that it provided much h^+ into the silicon. In the meanwhile, the silicon still dissolved near the interface of Ag/Si at a low rate because it could not consume that much, then those superfluous h^+ spread over the interface to enlarge holes. Furthermore, If H_2O_2 concentration is sufficiently high, the concentration of Ag^+ ions nearby the interface is also higher that cannot be 100% reduced into Ag nanoparticles, then some of these Ag^+ ions may shed into the solution and start to nucleate when saturated on the sidewall of previous holes, forming secondary Ag particles for new etch pathway and resulting in the porosification of Si.



Figure. 7 Spark from the moment of explosion

As described from the article about energetic PS [30, 31], which introduced that PS incorporate oxidizer can explode electric current or heating. It was found that the

explosion process of the porous silicon chip had obvious spark shown in Figure.7 and the sound of the explosion could be heard due to violent exothermic reactions, generated from unique porous structure characteristics with oxidant.

4. Conclusion

In summary, the experiment results indicated PS can be obtained from the SACE method, and these PS proved energetic when combined with oxidant as well. Moreover, this paper presents an approach for the Si etching structures by optimizing Ag nanoparticles distribution and H₂O₂ concentration. So we demonstrated that the SACE method provided the possibility of enabling controllable fabrication of silicon nanostructures for various potential applications, which is characterized by simple, convenient and low cost. From the research, we anticipate that this work might be useful for the researchers to fabricate desirable nanostructures. Significantly, the results of this research may serve as useful information when further experiments of the method are conducted and implemented in practical applications.

Conflict of interest

The authors declare no conflict of interest.

References

- [1] A. Uhler, Jr., Electrolytic Shaping of Germanium and Silicon, *Bell System Technical Journal* 35 (1956) 333-347.
- [2] W.R. Erwin, L. Oakes, S. Chatterjee, H.F. Zarick, C.L. Pint, R. Bardhan, Engineered Porous Silicon Counter Electrodes for High Efficiency Dye-Sensitized Solar Cells, *ACS Applied Materials & Interfaces* 6 (2014) 9904-9910.
- [3] L.-S. Jiao, J.-Y. Liu, H.-Y. Li, T.-S. Wu, F. Li, H.-Y. Wang, L. Niu, Facile synthesis of reduced graphene oxide-porous silicon composite as superior anode material for lithium-ion battery anodes, *Journal of Power Sources* 315 (2016) 9-15.
- [4] G. Barillaro, A. Diligenti, G. Marola, L.M. Strambini, A silicon crystalline resistor with an adsorbing porous layer as gas sensor, *Sensors and Actuators B: Chemical* 105 (2005) 278-282.
- [5] M. Li, M. Hu, D. Jia, S. Ma, W. Yan, NO₂-sensing properties based on the nanocomposite of n-WO_{3-x}/n-porous silicon at room temperature, *Sensors and Actuators B: Chemical* 186 (2013) 140-147.
- [6] F.V. Mikulec, J.D. Kirtland, M.J. Sailor, Explosive Nanocrystalline Porous Silicon and Its Use in Atomic Emission Spectroscopy, *Adv Mater* 14 (2002) 38-41.
- [7] S.K. Lazaruk, A.V. Dolbik, V.A. Labunov, V.E. Borisenko, Combustion and explosion of nanostructured silicon in microsystem devices, *Semiconductors+* 41 (2007) 1113-1116.
- [8] L. Currano, W. Churaman, Energetic Nanoporous Silicon Devices, *Microelectromechanical Systems, Journal of* 18 (2009) 799-807.

- [9] D. Dimova-Malinovska, M. Sendova-Vassileva, N. Tzenov, M. Kamenova, Preparation of thin porous silicon layers by stain etching, *Thin Solid Films* 297 (1997) 9-12.
- [10] X. Li, P.W. Bonn, Metal-assisted chemical etching in HF/H₂O₂ produces porous silicon, *Applied Physics Letters* 77 (2000) 2572-2574.
- [11] Z. Huang, N. Geyer, P. Werner, J. De Boor, U. Gösele, Metal-assisted chemical etching of silicon: A review, *Adv Mater* 23 (2011) 285-308.
- [12] C. Chartier, S. Bastide, C. Lévy-Clément, Metal-assisted chemical etching of silicon in HF–H₂O₂, *Electrochimica Acta* 53 (2008) 5509-5516.
- [13] N. Geyer, B. Fuhrmann, Z. Huang, J. de Boor, H.S. Leipner, P. Werner, Model for the Mass Transport during Metal-Assisted Chemical Etching with Contiguous Metal Films As Catalysts, *The Journal of Physical Chemistry C* 116 (2012) 13446-13451.
- [14] A.I. Hochbaum, R. Chen, R.D. Delgado, W. Liang, E.C. Garnett, M. Najarian, A. Majumdar, P. Yang, Enhanced thermoelectric performance of rough silicon nanowires, *Materials for Sustainable Energy* 2008, pp. 111-115.
- [15] H. Han, Z. Huang, W. Lee, Metal-assisted chemical etching of silicon and nanotechnology applications, *Nano Today* 9 (2014) 271-304.
- [16] M. Li, Y. Li, W. Liu, L. Yue, R. Li, Y. Luo, M. Trevor, B. Jiang, F. Bai, P. Fu, Y. Zhao, C. Shen, J.M. Mbengue, Metal-assisted chemical etching for designable monocrystalline silicon nanostructure, *Materials Research Bulletin* 76 (2016) 436-449.
- [17] K. Peng, J. Zhu, Simultaneous gold deposition and formation of silicon nanowire arrays, *Journal of Electroanalytical Chemistry* 558 (2003) 35-39.
- [18] M. Sainato, L.M. Strambini, S. Rella, E. Mazzotta, G. Barillaro, Sub-Parts Per Million NO₂ Chemi-Transistor Sensors Based on Composite Porous Silicon/Gold Nanostructures Prepared by Metal-Assisted Etching, *ACS Applied Materials & Interfaces* 7 (2015) 7136-7145.
- [19] K. Peng, Y. Xu, Y. Wu, Y. Yan, S.-T. Lee, J. Zhu, Aligned Single-Crystalline Si Nanowire Arrays for Photovoltaic Applications, 1 (2005) 1062-1067.
- [20] C.Y. Chen, C.S. Wu, C.J. Chou, T.J. Yen, Morphological Control of Single-Crystalline Silicon Nanowire Arrays near Room Temperature, *Adv Mater* 20 (2008) 3811-+.
- [21] J.-M. Chen, C.-Y. Chen, C.P. Wong, C.-Y. Chen, Inherent formation of porous p-type Si nanowires using palladium-assisted chemical etching, *Applied Surface Science* 392 (2017) 498-502.
- [22] K. Tsujino, M. Matsumura, Helical nanoholes bored in silicon by wet chemical etching using platinum nanoparticles as catalyst, *Electrochim Solid St* 8 (2005) C193-C195.
- [23] B. Wiley, Y. Sun, Y. Xia, Synthesis of Silver Nanostructures with Controlled Shapes and Properties, *Accounts of Chemical Research* 40 (2007) 1067-1076.
- [24] R. Zhang, A. Khalizov, L. Wang, M. Hu, W. Xu, Nucleation and Growth of Nanoparticles in the Atmosphere, *Chemical reviews* 112 (2011) 1957-2011.
- [25] T.M. Dung Dang, T.T. Tuyet Le, E. Fribourg-Blanc, M.C. Dang, Influence of surfactant on the preparation of silver nanoparticles by polyol method, *Advances in Natural Sciences: Nanoscience and Nanotechnology* 3 (2012) 035004.

- [26] J. Liu, X. Li, X. Zeng, Silver nanoparticles prepared by chemical reduction-protection method, and their application in electrically conductive silver nanopaste, *Journal of Alloys and Compounds* 494 (2010) 84-87.
- [27] Z. Zhang, B. Zhao, L. Hu, PVP Protective Mechanism of Ultrafine Silver Powder Synthesized by Chemical Reduction Processes, *Journal of Solid State Chemistry* 121 (1996) 105-110.
- [28] K.Q. Peng, A.J. Lu, R.Q. Zhang, S.T. Lee, Motility of Metal Nanoparticles in Silicon and Induced Anisotropic Silicon Etching, *Adv Funct Mater* 18 (2008) 3026-3035.
- [29] L. Kong, B. Dasgupta, Y. Ren, P. Katal Mohseni, M. Hong, X. Li, W. Chim, S. Chiam, Evidences for redox reaction driven charge transfer and mass transport in metal-assisted chemical etching of silicon, *Scientific Reports* 6 (2016).
- [30] D. Clément, D. Kovalev, *Nanosilicon-Based Explosives*, 2010.
- [31] L. Currano, W. Churaman, C. Becker, Nanoporous silicon as a bulk energetic material, *Solid-State Sensors, Actuators and Microsystems Conference*, 2009. *TRANSDUCERS 2009. International*, 2009.